2014 The Best of Basic Research

GLP-1 Receptor Localization in Monkey and Human Tissue: Novel Distribution Revealed With Extensively Validated Monoclonal Antibody

Charles Pyke, R. Scott Heller, Rikke K. Kirk, Cathrine Ørskov, Steffen Reedtz-Runge, Peter Kaastrup, Anders Hvelplund, Linda Bardram, Dan Calatayud, and Lotte Bjerre Knudsen

Department of Histology and Imaging (C.P., R.S.H., R.K.K.), Department of Incretin Biology (C.Ø.), Department of Diabetes Structural Biology (S.R.-R.), Department of Antibody Technology (P.K.), Department of Pharmaceutical Medicine Programme (A.H.), and Department of Diabetes and Pharmacology Management (L.B.K.), Novo Nordisk, 2880 Bagsværd, Denmark; and Department of Surgical Gastroenterology (L.B., D.C.), Rigshospitalet, 2100 Copenhagen Ø, Denmark

Glucagon-like peptide 1 (GLP-1) analogs are increasingly being used in the treatment of type 2 diabetes. It is clear that these drugs lower blood glucose through an increase in insulin secretion and a lowering of glucagon secretion; in addition, they lower body weight and systolic blood pressure and increase heart rate. Using a new monoclonal antibody for immunohistochemistry, we detected GLP-1 receptor (GLP-1R) in important target organs in humans and monkeys. In the pancreas, GLP-1R was predominantly localized in β-cells with a markedly weaker expression in acinar cells. Pancreatic ductal epithelial cells did not express GLP-1R. In the kidney and lung, GLP-1R was exclusively expressed in smooth muscle cells in the walls of arteries and arterioles. In the heart, GLP-1R was localized in myocytes of the sinoatrial node. In the gastrointestinal tract, the highest GLP-1R expression was seen in the Brunner's gland in the duodenum, with lower level expression in parietal cells and smooth muscle cells in the muscularis externa in the stomach and in myenteric plexus neurons throughout the gut. No GLP-1R was seen in primate liver and thyroid. GLP-1R expression seen with immunohistochemistry was confirmed by functional expression using in situ ligand binding with ^{125}I-GLP-1. In conclusion, these results give important new insight into the molecular mode of action of GLP-1 analogs by identifying the exact cellular localization of GLP-1R. (***Endocrinology*** **155: 1280–1290, 2014)**

Liraglutide and exenatide are approved for treatment of type 2 diabetes, and apart from lowering blood glucose, these glucagon-like peptide 1 (GLP-1) analogs also have a beneficial effect on body weight and blood pressure (BP). Furthermore, liraglutide is in phase 3 clinical development for the induction and maintenance of weight loss in people without diabetes who are obese. Both peptides selectively activate the GLP-1 receptor (GLP-1R), a G_s protein–coupled receptor (GPCR) (1). The expression of GLP-1R has been described in many tissues with the highest expression reported in the lung and pancreas and less expression in the stomach, intestine, kidney, heart, and brain (2–6). The liver has been reported to express GLP-1R, but recent publications do not show expression in hepatocytes in a study having rigorous controls (7). Several studies indicate that C-cells in the thyroid gland express GLP-1R; however, expression levels appear to be higher in rodents than in humans (8, 9). The exact cellular localization of the GLP-1R is poorly understood. In the pancreas, although it is well established that β-cells in the

ISSN Print 0013-7227 ISSN Online 1945-7170
Printed in U.S.A.

Received October 8, 2013. Accepted January 14, 2014.
First Published Online January 27, 2014

For News & Views see page 1175

Abbreviations: BP, blood pressure; DAB, diaminobenzidine; ECD, extracellular domain; GI, gastrointestinal; GLP-1, glucagon-like peptide 1; GLP-1R, GLP-1 receptor; GPCR, G protein–coupled receptor; HE, hematoxylin-eosin; HR, heart rate; IHC, immunohistochemistry; MAb, monoclonal antibody; PA, pulmonary artery; PDG, pancreatic duct gland; SAN, sinoatrial node; SMA, smooth muscle actin; SMC, smooth muscle cell; TBS, Tris-buffered saline.

islets of Langerhans are the main GLP-1R–expressing compartment, there are reports that other endocrine cells as well as ductal cells express GLP-1R (10–13). One of the main reasons for the sparse and conflicting information in the literature of the identity of GLP-1R–expressing cell types in vivo is the general problem with generating specific anti-GPCR antibodies that reliably detect such receptors in tissue sections using immunohistochemistry (IHC) (14–17). Recently, we and others have reported a problem with identifying specific antibodies for use in IHC and Western blotting for GLP-1R (7, 18). Here, extensive validation of a monoclonal GLP-1R antibody for IHC is reported, and this antibody is used for the specific and highly sensitive detection of GLP-1R in formalin-fixed and paraffin-embedded samples of primate pancreas, kidney, lung, heart, gastrointestinal (GI) tract, liver, and thyroid.

Materials and Methods

Generation of monoclonal anti-GLP-1R antibody

GLP-1R knockout mice were used for immunization with the human GLP-1R extracellular domain (ECD) refolded and purified as described previously (19) and conjugated to keyhole limpet hemocyanin. This strain of mice is on a C57BL background and is derived from the previously described GLP-1R knockout strain (20) custom bred by Novo Nordisk A/S at Taconic. The strain is not commercially available. The immunization protocol was approved by the Danish Animal Experiments Council and the Danish Ministry of Justice. Spleens from mice with positive serum titers were removed aseptically and dispersed to a single cell suspension. Spleen and myeloma cell fusions (P3X63Ag8.653, ATCC CRL-1580) were performed using the electrofusion method. Screening for GLP-1R ECD binding was performed by ELISA. A total of 11 positive clones were selected for testing by IHC.

Tissue preparation and sectioning

For preparation of paraffin-embedded tissue samples for IHC, *Macaca mulatta* (rhesus monkey) and *Macaca fascicularis* (cynomolgus monkey) and human tissue specimens were immersion fixed in 4% (w/v) paraformaldehyde in 0.1 M phosphate buffer (pH 7.4), for at least 24 hours at 4°C, and then were dehydrated and embedded in paraffin wax. Monkey necropsy and tissue handling were performed according to regulations specified under the Protection of Animals Act by the Authority in the European Union (directive 2010/63/EU). Pancreas samples were included from two normal cynomolgus monkeys and 7 normal and 7 diabetic rhesus monkeys. Whole-organ samples of the two cynomolgus monkey pancreata were sectioned systematically (4 μm) and stained with hematoxylin-eosin (HE) to identify areas of the main duct containing pancreatic duct glands (PDGs). A similarly thorough sampling was performed for the ampulla of Vater regions from both cynomolgus monkeys. Samples from kidney, lung, stomach, duodenum, jejunum, ileum, colon, liver, and thyroid from the 7 normal rhesus monkeys were included. Unfixed specimens from the same organs from rhesus monkeys were embedded in cryoprotectant, and frozen sections (10 μm) were cut for in situ ligand binding. For the studies of cynomolgus monkey heart tissue, paraffin-embedded sections were used, representing all areas from a male and a female monkey heart, as well as frozen sections, representing all areas from a male monkey.

Human pancreas tissue blocks from surgical resection specimens were obtained from the Department of Surgical Gastroenterology, Copenhagen University Hospital, Copenhagen, Denmark (n = 9) and from two commercial providers (Tissue Solutions, Clydebank, Scotland [n = 8] and Cambridge Bioscience, Cambridge, UK [n = 5]). Postmortem human normal heart (n = 1) sinoatrial node (SAN) tissue blocks were obtained from Tissue Solutions. Postmortem human normal kidney (n = 2) tissue blocks were obtained from BioServe Biotechnologies Ltd. The sampling and histological use of all human tissues were ethically approved by local authorities.

Preparation of GLP-1R transfected cell controls

Two baby hamster kidney (BHK) cell lines stably expressing the human GLP-1 receptor and characterized by high and low (21, 22) expression levels were used to test the reactivity of GLP-1R antibodies. Untransfected BHK cells were used as negative controls. Semiconfluent cultures were scraped, and the cells were spun down (5 minutes at 1200 $\times$ *g*), the supernatants were removed, and the pellets were fixed in 1% paraformaldehyde at 4°C overnight. The next day, cells were suspended in 60°C agar and transferred to 5-mm pieces of soft plastic tubing and then were allowed to gel at 4°C for 5 minutes. The agar cylinders were removed from the plastic tubing and embedded in paraffin.

IHC protocols

Single-label IHC diaminobenzidine (DAB) staining

Paraffin sections were dewaxed and rehydrated to double-distilled H_2O. Sections were microwave treated for 15 min in Tris-EGTA buffer (pH 9.0). Sections were allowed to cool for 15 to 30 minutes and rinsed in double-distilled H_2O and treated with 1% H_2O_2 in Tris-buffered saline (TBS) for 15 minutes. Slides were incubated in TBS overnight at 4°C. Slides were washed in TBS with 0.05% Tween (TBS-T) and blocked with 5% skimmed milk for 30 minutes, followed by incubation with the primary GLP-1R antibody (monoclonal antibody [MAb] 3F52) diluted in TBS with 0.5% skimmed milk for 2 hours at room temperature. Five washes in TBS-T for 5 minutes each were then followed by Flex+ Linker (Dako) for 20 minutes. The slides were again washed before the addition of Flex+/HRP for 15 minutes. Another wash was performed, and the slides were developed with DAB+ (Dako) and counterstained with HE, rinsed in water, dehydrated, and mounted.

Double-labeling fluorescence IHC

Paraffin sections were treated as above until incubation with MAb 3F52 at 1 μg/ml in TBS with 0.5% skimmed milk for 2 hours at room temperature. Slides were washed and then were incubated with the biotin-free catalyzed system amplification system (CSA II) with anti-mouse horseradish peroxidase (Dako) for 10 minutes. The slides were washed, followed by addition of the CSA II amplification reagent for 5 minutes. After washing, slides were blocked with 5% skimmed milk for 30 minutes, incubated with the second primary (rabbit) antibody for 60 minutes, washed, and incubated with Alexa 594–labeled donkey-anti-rabbit antibody. The rabbit antibodies used were reacting

with insulin (AP08860PU-N [Acris Antibodies GmbH] and C27C9 [Cell Signaling Technology Inc]), glucagon and calcitonin (A0565 and A0576, respectively; Dako), cytokeratin-19 (Ab15463; Abcam), renin (54371; AnaSpec), Cbl proto-oncogene, E3 ubiquitin protein ligase B (CBLB) and hyperpolarization-activated cyclic nucleotide-gated channel-4 (HCN4) (HPA019880 and H0284, respectively; Sigma-Aldrich), and smooth muscle actin (SMA) (Ab5694, Abcam). After washing, sections were stained with Hoechst nuclear stain for 10 minutes and rinsed in water for 1 minute before mounting. All sections were scanned in a NanoZoomer 2.0HT slide scanner (Hamamatsu), digital images were analyzed, and representative areas were used for the figures.

In situ ligand binding

In situ ligand binding for functional GLP-1R localization was performed as described previously, apart from the use of ^{125}I-GLP-1 (7–36) (NEX3080; PerkinElmer) instead of ^{125}I-exendin (9–39) (21, 22). The tracer was used at a concentration of 0.3 nM, and specificity was assessed by the coincubation with 100 nM unlabeled GLP-1.

Results

Identification of antibodies reactive with human GLP-1R after formalin fixation and paraffin embedding

To identify MAbs specific for GLP-1R and useful for detecting primate GLP-1R in tissue blocks, we first tested clones for reactivity for GLP-1R ECD used in immunization. We then screened 11 MAb clones for binding to the full-length human GLP-1R expressed in BHK cells, both as fresh frozen cells and as formalin-fixed and paraffin-embedded cells. We identified 4 clones that showed reactivity to human GLP-1R–transfected cells, with no reactivity to nontransfected cells. The same 4 clones also showed membrane-associated reactivity with islet cells in formalin-fixed and paraffin-embedded monkey pancreas, and one clone, MAb 3F52, was selected for further studies because of its superior signal to noise ratio in both transfected cells and pancreas tissue (18). We tested MAb 3F52 in 2 different IHC protocols and found that the 2 methods yielded identical results and had comparable sensitivity, confirming that we could use this antibody in a double-labeling protocol for better cell identification (Supplemental Figure 1A published on The Endocrine Society's Journals Online web site at http://end.endojournals.org). MAb 3F52 was also shown to detect GLP-1R in Western blotting using peptide-*N*-glycosidase F–treated lysates from BHK cells transfected with human GLP-1R (Supplemental Figure 1B). When tested on cells transfected with rabbit and mouse GLP-1R, no reactivity with MAb 3F52 was detected, indicating that this antibody is primate specific (Supplemental Figure 1B and data not shown). The epitope reactivity of MAb 3F52 was determined by crystallization of the Fab region with human GLP-1R ECD, and Trp33 was found to be the main determinant of species specificity (Reedtz-Runge, S., unpublished information). With this information and using the National Center for Biotechnology Information protein blast tool, we determined that the only published GLP-1R sequences with tryptophan in position 33 are from primate species. In contrast, GLP-1R from mouse, rat, goat, rabbit, pig, cow, cat, and dog are all predicted to be nonreactive with MAb 3F52.

Normal primate kidney

IHC with MAb 3F52 on frozen sections of cynomolgus monkey kidney yielded a distinct signal exclusively in the preglomerular vascular compartment, ie, in vas afferens arterioles, interlobular arteries, and arcuate arteries (Supplemental Figure 2, A–C). This binding was specific as determined by the absence of reactivity with an isotype control antibody at the same concentration (Supplemental Figure 2, D–F). The specificity of MAb 3F52 was further validated by demonstrating complete overlap of the MAb 3F52 IHC signal with the ISLB signal for functional GLP-1R using ^{125}I-GLP-1 on adjacent frozen sections (Supplemental Figure 2, G–I). The GLP-1R ISLB signal could be completely inhibited with the coincubation of excess unlabeled GLP-1 (Supplemental Figure 2, J–L). IHC with MAb clone 3F52 on paraffin-embedded normal monkey kidney sections showed the exact same pattern of immunoreactivity with selective labeling of vas afferens arterioles, interlobular arteries, and arcuate arteries in the kidney. The immunoreactivity was located exclusively in the smooth muscle cells (SMCs) in the wall of the GLP-1R–positive arterioles and arteries, whereas the endothelial cell layer was negative (Figure 1A). The staining was both membrane-associated and cytoplasmic. No other cells or compartments in the kidney, including glomeruli and tubuli, showed a signal (Figure 1A). To determine whether some or all of the GLP-1R–expressing cells were juxtaglomerular cells, double-labeling IHC for renin and GLP-1R was conducted. This demonstrated that the GLP-1R–expressing SMCs in vas afferens arterioles were closely associated with juxtaglomerular cells, and frequently the same cells stained for renin and for GLP-1R (Figure 1, B and C).

On the basis of these data, we concluded that MAb 3F52 was fully validated for use in IHC. In 2 postmortem samples of normal human kidney using MAb 3F52, we observed an expression pattern of GLP-1R that was very similar to that seen in monkey kidneys. In the cortex of these kidneys, only SMCs in the arterial and arteriolar walls showed immunoreactivity (data not shown).

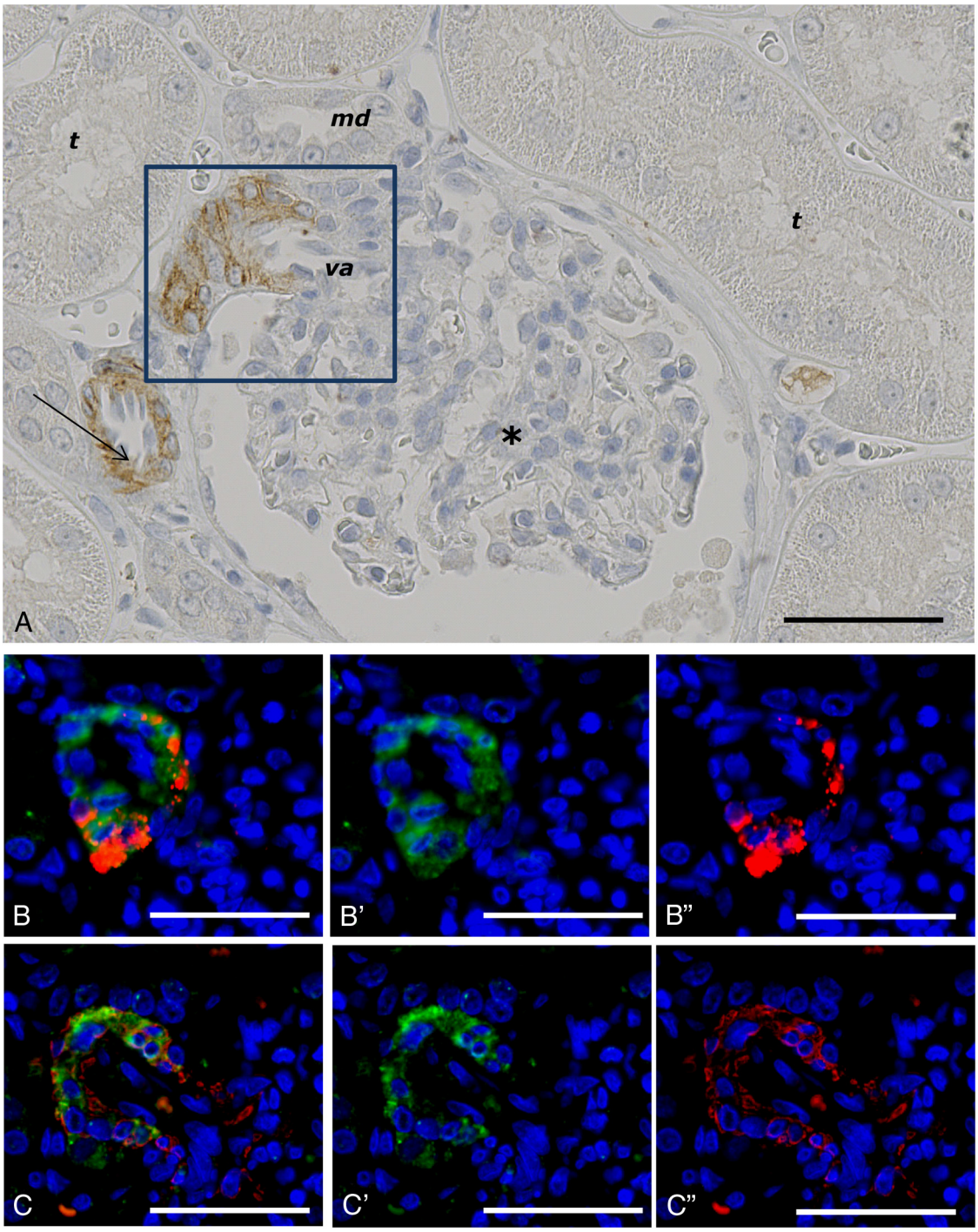

Figure 1. A, GLP-1R immunoreactivity in smooth muscle cells of a vas afferens (va) arteriole at the vascular pole. Note the absence of signal in the macula densa (md), tubuli (t), glomerulus (*), and endothelial cells within an arteriole (arrow). B and C, Near-adjacent sections showing double labeling for GLP-1R (green)/renin (red) and GLP-1R (green)/SMA (red), respectively. B′ and C′, Same as B and C, respectively, with red fluorescence digitally removed to highlight GLP-1R immunoreactivity. B″ and C″, Same as B and C, respectively, with green fluorescence digitally removed to highlight renin and SMA immunoreactivity, respectively. Scale bars correspond to 50 μm.

Normal monkey pancreas

Using paraffin-embedded samples of normal monkey pancreas, DAB IHC was performed with MAb 3F52. Prominent immunoreactivity was consistently seen in the islets of Langerhans (Figure 2, A–C), and this staining was predominantly membrane associated (Figure 2C). With use of a fluorescence double-labeling protocol, complete colocalization of GLP-1R and insulin-reactive cells was seen (Figure 2E). In double-labeling IHC with MAb 3F52 and antibodies reactive with glucagon, somatostatin, and pancreatic polypeptide, GLP-1R expression was not present in the large majority of non–β-endocrine islet cells,

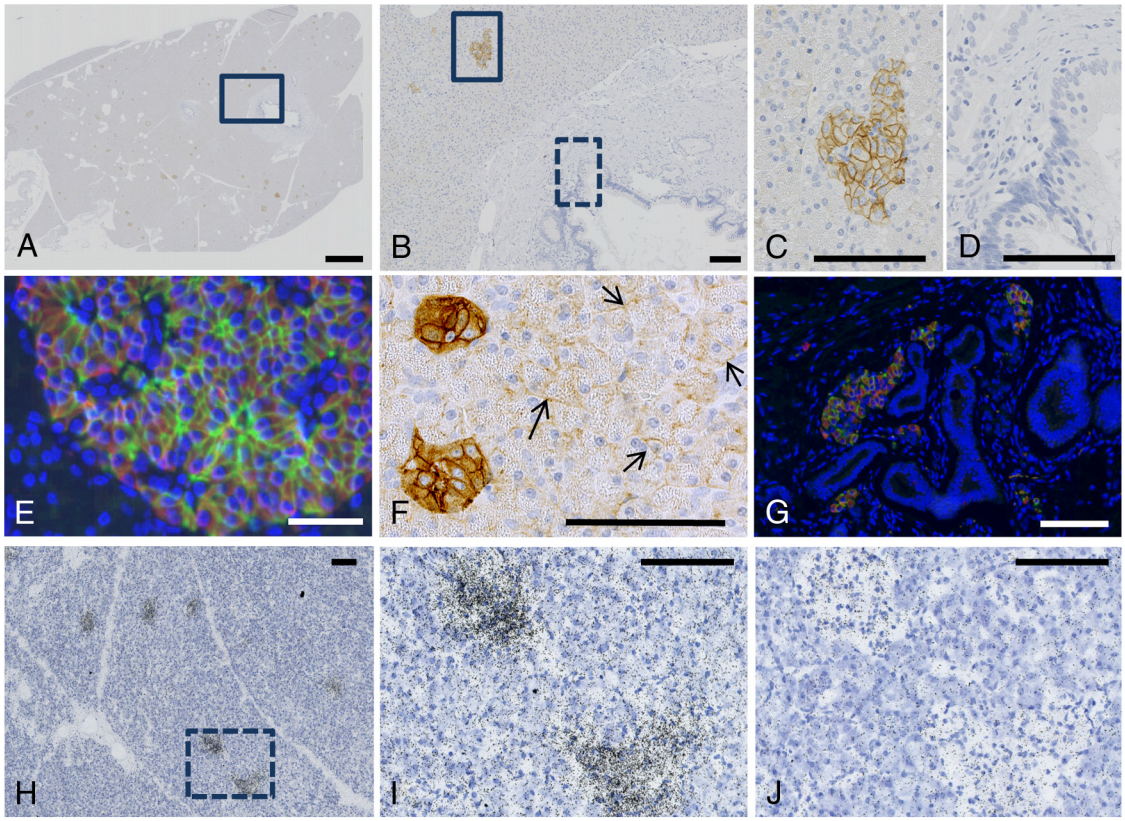

Figure 2. GLP-1R IHC with antibody MAb 3F52 on paraffin-embedded monkey pancreas (A–G) and ISLB with ^{125}I-GLP-1 on a frozen section from monkey pancreas (H–J). B and C, Magnifications of solid-line boxed areas in A and B, respectively. D, High magnification of the dashed-line boxed area in B. I, High magnification of the boxed area in H. A–D and F, GLP-1R immunoreactivity using a DAB IHC protocol. E and G, Images from a double-labeling GLP-1R/insulin IHC fluorescence protocol. In E, double labeling for GLP-1R (green) and insulin (red) shows complete colocalization, demonstrating that all GLP-1R–positive cells are β-cells. The ductal epithelium is negative for GLP-1R (D). In F, weakly GLP-1R–immunopositive acinar cells (arrows) can be seen adjacent to strongly staining islets (left). G, High-magnification image of the main duct area of a cynomolgus monkey pancreas double-immunostained for GLP-1R (green) and insulin (red). J, Image from the section adjacent to I and incubated with ^{125}I-GLP-1 plus an excess of unlabeled GLP-1. Scale bars correspond to 1 mm (A) and 100 μm (B–J).

although the close proximity of endocrine cells in islets made it impossible to exclude the possibility that rare endocrine GLP-1R–positive non–β-cells could be present (Supplemental Figure 3, A–F).

Apart from β-cells, acinar cells showed variable and always markedly weaker GLP-1R immunoreactivity than β-cells (Figure 2F). GLP-1R staining with MAb 3F52 was never observed in ductal epithelial cells (Figure 2D). To specifically analyze the expression of GLP-1R in the main duct of the monkey pancreas, we prepared sections from all levels of the proximal main pancreatic duct from two cynomolgus monkeys. For every 50 μm, two adjacent sections were immunostained for GLP-1R/insulin and GLP-1R/cytokeratin-19, to allow an assessment of whether ductal epithelial cells were positive for GLP-1R. In all of the sections investigated from both animals, we detected GLP-1R only in insulin-producing cells, as determined by the colocalization with insulin (Figure 2G). With Alcian Blue and periodic acid–Schiff staining to identify PDGs, distinct gland-like mucinous compartments reported to be present in rodent and primate pancreas (23), we were unable to confirm the presence of PDGs in any sections from any of the monkey main pancreatic duct samples.

With use of ISLB for detection of functional GLP-1R on frozen samples of normal monkey pancreas, a pronounced signal was seen in all islets (Figure 2, H–I). Apart from this signal, a markedly weaker signal was observed in acinar cells. The signal in both islets and acinar cells could be displaced by an excess of unlabeled GLP-1 and by the addition of MAb 3F52 but not by the addition of an isotypic control MAb (Figure 2J and Supplemental Figure 3I). This control experiment further supported the theory that the ^{125}I-GLP-1 binding seen in both islets and acinar cells is to the known GLP-1R.

Apart from islet endocrine cells and acinar cells, no other cells in the monkey pancreas displayed ^{125}I-GLP-1 binding activity or an IHC signal, including ductal epithelial cells, endothelial cells, fibroblasts, stellate cells, or any other nonacinar cells in the exocrine compartment.

Normal human pancreas

IHC for GLP-1R with MAb 3F52 was performed on a total of 10 human pancreas surgical resection specimens

that were from nondiabetic individuals; the histological appearance was within the normal range, although some samples showed evidence of fibrosis and inflammatory cell infiltration (Supplemental Table 1). The pattern of GLP-1R immunoreactivity was similar to that seen in the normal monkey pancreas samples. In double-labeling fluorescence GLP-1R/insulin IHC, we verified the complete colocalization of the two proteins in islets and islet-like structures in all human pancreas samples (Figure 3, A–C). Coexpression of GLP-1R and insulin was seen occasionally in cells located in aberrant foci in approximately half of the human pancreas samples. These foci were morphologically compatible with neodifferentiation of islets of Langerhans from pancreatic exocrine duct epithelium or ductulo-insular complexes (Figure 3J). Similarly to the normal monkey pancreas, acinar cells showed variable but always markedly weaker GLP-1R immunoreactivity compared with that of β-cells.

As was the case for monkey pancreas, we never observed staining of ductal epithelial cells (Supplemental Figure 4). Using Alcian Blue and periodic acid–Schiff staining to highlight PDGs in all the human pancreas samples, we were able to demonstrate these structures in 2 of the human samples, and in these, we saw no GLP-1R immunoreactivity (Figure 3, G–I).

Diabetic monkey pancreas

GLP-1R IHC with MAb 3F52 was performed on a set of 7 type 2 diabetic rhesus monkey pancreas samples, and in all samples we detected GLP-1R in islets and islet-like structures, As was seen in the set of the 7 normal rhesus pancreas samples, in all 7 diabetic rhesus pancreas samples there was complete overlap between GLP-1R– and insulin-expressing cells, and, consequently, in the pancreas samples from diabetic individuals there were markedly fewer GLP-1R–positive islets and endocrine cells than in the 7 normal samples (Supplemental Figure 3, G–H). Weak GLP-1R immunoreactivity was observed in acinar cells, with no difference detected in frequency and staining intensity between normal and diabetic samples. Ductal

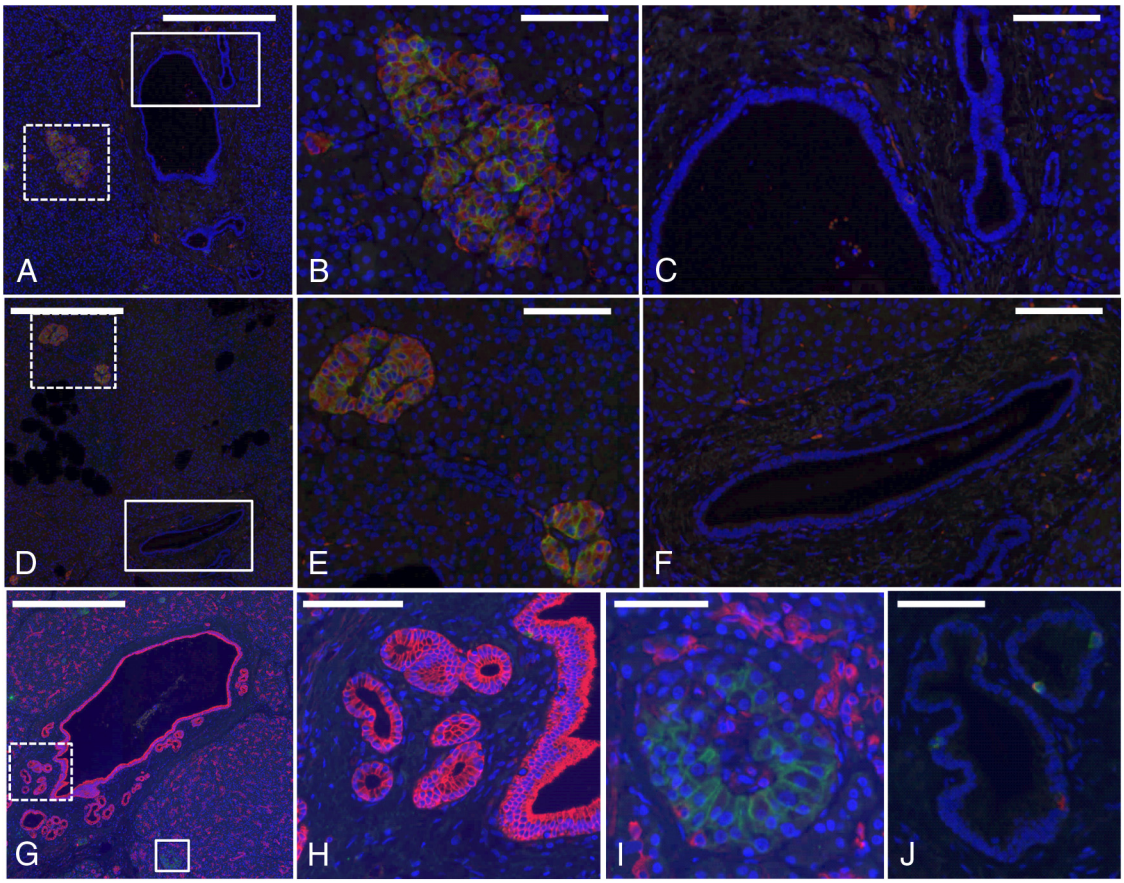

Figure 3. A normal (A–C and G–J) and a diabetic (D–F) human pancreas double labeled for GLP-1R (green) and insulin (red). B and E, High-magnification images of the dashed-line boxes in A and D, respectively. C and F, High-magnification images of the solid-line boxes in A and D, respectively. Note the complete colocalization of signals for GLP-1R and insulin in islets in A, B, D, and E and absence of staining of ductal epithelium in C and F. G–I, GLP-1R (green)/cytokeratin-19 (red) double staining in sample of normal human pancreas containing part of the main duct with PDGs. G, Low-magnification overview. H, High magnification of area (dashed-line box in G) containing PDGs and showing no GLP-1R immunoreactivity. I, High magnification of area (solid line box in G) containing an islet with GLP-1R immunoreactive β-cells. J, Two GLP-1R/insulin–positive cells are located within the ductal epithelium. Scale bars correspond to 0.5 mm (A, D, and G), 100 μm (B, C, E, F, H, and J), and 50 μm (I).

epithelial cells were always negative, including all parts of the main duct present in 6 of the 7 diabetic and 6 of the 6 normal samples (Supplemental Figure 3, G–H).

Diabetic human pancreas

As was the case for diabetic monkey pancreas samples, in the 12 pancreas samples from human diabetic individuals, there was complete colocalization of GLP-1R and insulin in islets and islet-like structures in all human pancreas samples, a weak staining for GLP-1R in acinar cells, and an absence of GLP-1R staining of ductal epithelial cells (Figure 3, D–F, and Supplemental Figure 4). As in the normal human pancreas samples, GLP-1R and insulin colocalization was occasionally observed in aberrant islet-like foci (Supplemental Figure 4W). No other immunoreactive cells were observed in the monkey and human diabetic pancreas samples.

Normal primate heart

IHC with MAb 3F52 on sections representing all areas of three normal monkey hearts revealed moderately strong GLP-1R immunoreactivity exclusively in the myocytes of the SAN (Figure 4). Control experiments included staining

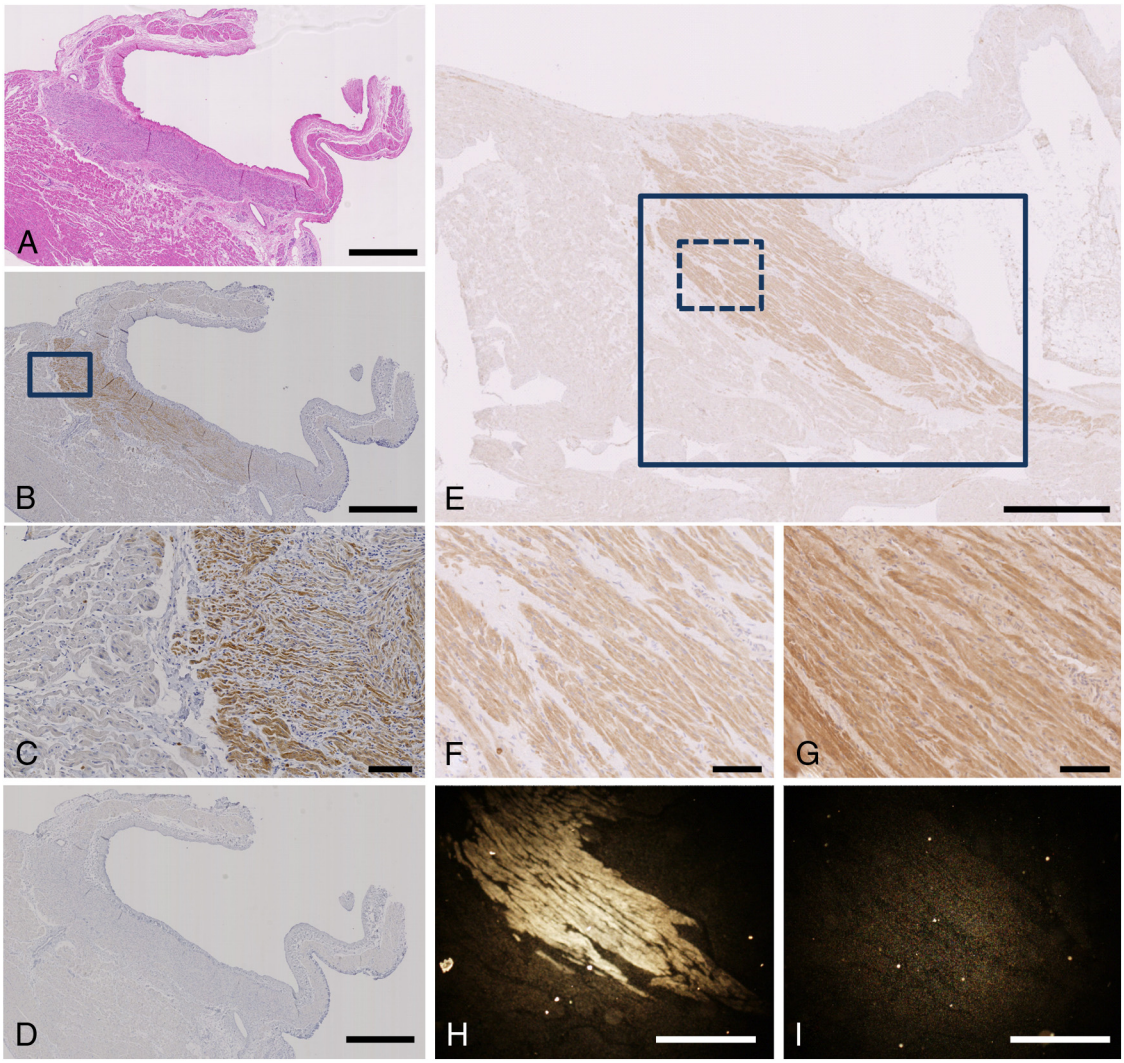

Figure 4. Identification of GLP-1R immunoreactive cells in the monkey heart as SAN myocytes. A, HE section of paraffin-embedded monkey heart containing the SAN region. B, Adjacent section immunostained for GLP-1R with MAb 3F52 show exclusive reactivity to SAN myocytes (seen as brown DAB staining). C, High magnification of boxed area in B to highlight GLP-1R immunopositive SAN myocytes (right) juxtaposed to nonreactive cardiomyocytes lying outside of the SAN (left). D, Section adjacent to B and reacted with isotype control antibody at the same concentration. E–I, Validation of GLP-1R immunoreactive cells being SAN myocytes. IHC for HCN4 (a marker of SAN myofibers) (E and F) and GLP-1R with MAb 3F52 (G) on adjacent frozen sections from a monkey heart. F, High-magnification image of the dashed-line box in E. G, GLP-1R–immunoreactive SAN myocytes from same area as F. H, In situ ligand binding with ^{125}I- GLP-1 on frozen section adjacent to G. Note that the area in H, similar to the solid-line box in E, shows a prominent autoradiography signal completely overlapping with GLP-1R– and HCN4-immunopositive SAN myocytes. The image is darkfield to highlight the positive signal. I, Darkfield image of same area as in H showing the section adjacent to H and incubated with ^{125}I-GLP-1 plus an excess of unlabeled GLP-1, demonstrating the specificity of binding in H. Scale bars corresponding to 1 mm (A, B, D, E, H, and I) and 100 μm (C, F, and G).

for the hyperpolarization-activated cyclic nucleotide–gated channel-4(HCN4) in adjacent sections (Figure 4, E–G) and ISLB with ^{125}I-labeled GLP-1 (Figure 4H). The atrioventricular node, other atrial and ventricular myocytes, the HIS-Purkinje system, SMCs, and endothelial cells did not show GLP-1R staining.

The selective localization of GLP-1R in the SAN region of the monkey heart prompted us to investigate a paraffin-embedded specimen of human heart SAN region with IHC using MAb 3F52. In this sample, we confirmed SAN myocyte GLP-1R immunoreactivity (Supplemental Figure 5).

Normal monkey GI tract

Monkey GI samples representing the stomach, duodenum with Brunner's gland, jejunum, ileum, and colon were stained for GLP-1R using MAb 3F52. In the stomach, moderately intense staining for GLP-1R was seen in a subset of the parietal cells and weak staining in a subset of SMCs in the muscularis externa (Figure 5A and Supplemental Figure 6, A–C). In the duodenum, prominent GLP-1R staining was seen in Brunner's gland epithelium, with a predominant basolateral membrane-associated staining of epithelial cells (Supplemental Figure 6, J–K). Apart from this localization, a low-intensity GLP-1R signal was present in the myenteric nerve plexus in all gut segments (Supplemental Figure 6, E–I). The IHC signals in the GI tract were validated with ISLB using ^{125}I-labeled GLP-1 (Supplemental Figure 6, L–M).

Tissue-infiltrating mast cells showed immunoreactivity in paraffin-embedded tissue but not in frozen tissue (not shown). This cell population is known to give rise to unspecific binding of antibodies (24).

Normal monkey lung

IHC with MAb 3F52 on sections from normal rhesus monkey lung showed weak but specific GLP-1R immunoreactivity in pulmonary artery (PA) branches in the smooth muscle cell layer (Figure 5B).

Normal monkey thyroid

We did not detect GLP-1R immunoreactivity in any normal monkey thyroid samples. To confirm that C cells were present in the samples, we performed IHC for calcitonin on adjacent sections. This staining very clearly identified C cells in all samples, and these were in all cases negative for GLP-1R (Figure 6).

Normal monkey liver

We detected no IHC signal with MAb 3F52 in any normal monkey liver samples (data not shown).

Discussion

Several reports of the mapping of GLP-1R–expressing cells in selected organs have been published during recent

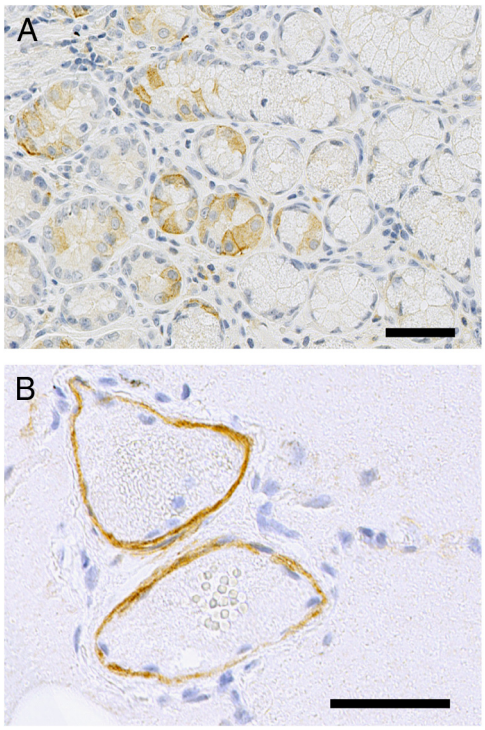

Figure 5. A, In the normal monkey stomach, a subset of parietal cells (identified by positive immunoreactivity with anti-CBLB) display mainly membrane-associated GLP-1R immunoreactivity. B, GLP-1R immunoreactivity is seen in smooth muscle cells in the wall of a PA in monkey lung. Scale bars correspond to 50 μm.

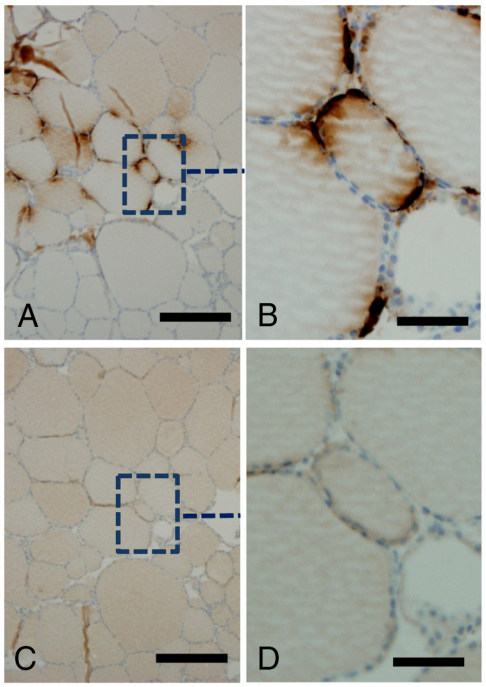

Figure 6. IHC staining with MAb 3F52 and polyclonal anti-calcitonin antibody A0576 of normal monkey thyroid tissue. A and B, Anti-calcitonin, 1 μg/ml. C and D, MAb 3F52. Note that C cells do not express GLP-1R. Scale bars correspond to 100 μm.

years, but a comprehensive description of GLP-1R–expressing cell types in the major GLP-1 target organs is not available in the literature. Further complicating matters are several examples of species differences between rodents and humans (8) as well as the use of unvalidated histological methods. Using a specific anti-GLP-1R MAb in 2 different IHC protocols selected for their high sensitivity on paraffin-embedded human and monkey tissues, in the present study we documented the identity of GLP-1R–expressing cells in 5 major GLP-1 target organs: kidney, pancreas, heart, lung, and GI tract (Table 1). ISLB was used for validating the specificity of MAb 3F52 and, in combination, the data constitute strong evidence for the presence of functional GLP-1R in the organs and cells where immunoreactivity was detected.

No GLP-1R immunoreactivity was detected in normal monkey thyroid and liver. In normal human thyroid samples, an independent group working with MAb 3F52 for IHC studies did not observe GLP-1R expression in normal-appearing human thyroid samples (Reubi, J.C., personal communication).

In the pancreas, the main GLP-1R–containing compartments are β-cells with a consistently strong and predominantly membrane-associated immunoreactivity in all insulin-producing cells in normal human and monkey pancreas. The low-level GLP-1R expression in acinar cells reported in this study corresponds well with previous reports using ISLB on normal human pancreas (8, 25). GLP-1R expression was not observed in duct epithelial cells in a total of 22 human and 16 monkey samples from both normal and diabetic pancreata. Again, this result is in agreement with the results of ISLB studies of human pancreas samples in which the presence of GLP-1R in ductal compartments was never observed (Reubi, J.C., personal communication). In an IHC study with another anti-GLP-1R antibody in human paraffin-embedded samples from nonneoplastic pancreata adjacent to surgically resected pancreatic cancer (13), the authors reported that GLP-1R was readily detected in PDGs and pancreatic intraepithelial neoplasias, with less staining of normal-appearing ducts. In view of recently published data reporting that a range of polyclonal anti-GLP-1R antibodies cannot be used to detect GLP-1R in IHC or Western blotting (7, 18) and with no validation of antibody specificity in paraffin-embedded tissues, we find it unlikely that the IHC protocol and antibody used in the study by Gier et al (13) had the necessary specificity to detect GLP-1R in human archival material. After recent changes in the editorial guidelines for publication of antibody-based data by this journal (26) and a recent review published in *Diabetes* that challenges the specificity of the antibodies used and some of the results obtained (27), it seems prudent to suggest that IHC data for GPCRs should always be extensively validated, eg, by demonstrating colocalization of signals with a non–antibody-based technique such as ISLB or in situ hybridization.

The exclusive expression of GLP-1R in the vascular wall of arterioles and arteries in the kidney supports a

Table 1. Summary of GLP-1R Localization in Normal Monkey Using IHC with MAb 3F52

Organ	Identity of GLP-1R$^+$ Cells	Staining Intensity	Potential Direct Physiological Role
Pancreas	β-cells	+++	↑ Insulin secretion
	Acinar cells	+	↑ Lipase secretion
Stomach	Parietal cells	++	↓ Gastric acid secretion
	Muscle cells	+	↓ Gastric emptying
Duodenum	Brunner's gland epithelial cells	+++	↑ Mucus secretion
	Myenteric plexus neurons	+	↓ Intestinal motility
Jejunum, ileum, colon	Myenteric plexus neurons	+	↓ Intestinal motility
Lung	Pulmonary artery SMCs	+	↓ Vascular resistance
Kidney	Arterial/arteriolar SMCs	++	↑ Glomerular filtration rate ↓ BP
Heart	Sinoatrial node myocytes	+	↑ HR ↓ BP
Liver	No staining		None
Thyroid	No staining		None

physiological role for GLP-1 in this target organ to induce dilation of vessels supplying the glomeruli as suggested previously (8, 28–30). Even though BP reduction is a well-described effect of GLP-1R agonists (31), the mechanism is not fully established, and our data on GLP-1R localization in the kidney do not directly provide an explanation for this effect. In this respect, it is interesting that GLP-1R expression is consistently observed in renin-secreting cells of the juxtaglomerular apparatus. A recent study in normal human volunteers reported a significant effect on natriuresis but no change in renin secretion with a 2-hour iv infusion of GLP-1, indicating that GLP-1–mediated effects on renin secretion are not directly implicated in the BP-lowering effect of GLP-1 (32). Another recent study demonstrated that GLP-1–induced atrial natriuretic peptide secretion is a physiological mediator of the BP reduction induced by GLP-1 in mice (33). The latter article also discusses whether the BP-lowering effects could be mediated by a combination of renal and cardiac effects, and GLP-1R was found in that article to be predominantly expressed in the atrial region of the mouse heart. The present data add the important fact that in primates the GLP-1R is expressed by SAN myocytes. GLP-1 has been reported to increase heart rate (HR), and it is possible that GLP-1–mediated stimulation of GLP-1R on SAN myocytes could explain, at least in part, the HR increase and potentially also the BP effect of the GLP-1 class drugs. It should be noted that GLP-1R–expressing neurons in the brain could also be responsible for GLP-1 effects on water and salt homeostasis (34, 35).

Similarly to that in the kidney, GLP-1R immunoreactivity was expressed in lung SMCs of PA branches. As noted above for the GLP-1R–expressing preglomerular arterioles in the kidney, it is conceivable that GLP-1R in the lung has a physiological role in regulating postprandial vascular tone, but functional evidence to support this role is lacking. Interestingly, a significant species difference seems to exist for lung expression with rodent lung expressing a very high level of GLP-1R in both vessels and alveolar epithelium, whereas in human lung GLP-1R is expressed only in the vascular tree (8).

In the normal monkey GI tract, we found prominent GLP-1R expression in Brunner's gland epithelial cells in the duodenum and weaker expression in myenteric plexus neurons throughout the GI tract. This localization is similar to previously reported data using ISLB on normal human tissue samples (8). In the stomach, a subset of both parietal cells and muscle cells of the muscularis externa were immunopositive for GLP-1R. GLP-1 has been shown to inhibit gastric acid secretion and gastric motility (36), and these effects fit well with our GLP-1R IHC findings.

In conclusion, we have generated and validated the specificity of a highly sensitive and specific MAb and have applied this antibody in a thorough characterization of primate GLP-1 target organs. In the case of the pancreas, previous data were essentially confirmed but careful evaluation of GI, cardiac, and renal tissues revealed completely novel cellular localizations of importance for the full understanding of basic GLP-1 physiology and potentially also relevant for interpretation of clinical effects among the growing pool of patients with type 2 diabetes who are being treated with GLP-1R agonists.

Acknowledgments

The excellent technical assistance of Pia G. Mortensen, Bettina Brandrup, Charity M. K. Graae, and Maibritt C. Pedersen is gratefully acknowledged. Nikolaj Kulahin is gratefully acknowledged for providing Western blotting control.

Address all correspondence and requests for reprints to: Lotte Bjerre Knudsen, Novo Nordisk, Novo Nordisk Park, DK-2760 Maaloev, Denmark. E-mail: lbkn@novonordisk.com.

Disclosure Summary: C.P., R.S.H., R.K.K., C.Ø, S.R.-R., P.K., A.H., and L.B.K. are full-time employees of Novo Nordisk A/S, which markets liraglutide for the treatment of diabetes and hold minor stock portions as part of an employee offering program. L.B. and D.C. have nothing to disclose.

References

1. **Brubaker PL, Drucker DJ.** Structure-function of the glucagon receptor family of G protein-coupled receptors: the glucagon, GIP, GLP-1, and GLP-2 receptors. *Receptors Channels*. 2002;8:179–188.
2. **Thorens B.** Expression cloning of the pancreatic β cell receptor for the gluco-incretin hormone glucagon-like peptide 1. *Proc Natl Acad Sci USA*. 1992;89:8641–8645.
3. **Campos RV, Lee YC, Drucker DJ.** Divergent tissue-specific and developmental expression of receptors for glucagon and glucagon-like peptide-1 in the mouse. *Endocrinology*. 1994;134:2156–2164.
4. **Bullock BP, Heller RS, Habener JF.** Tissue distribution of messenger ribonucleic acid encoding the rat glucagon-like peptide-1 receptor. *Endocrinology*. 1996;137:2968–2978.
5. **Dunphy JL, Taylor RG, Fuller PJ.** Tissue distribution of rat glucagon receptor and GLP-1 receptor gene expression. *Mol Cell Endocrinol*. 1998;141:179–186.
6. **Wei Y, Mojsov S.** Tissue-specific expression of the human receptor for glucagon-like peptide-I: brain, heart and pancreatic forms have the same deduced amino acid sequences. *FEBS Lett*. 1995;358:219–224.
7. **Panjwani N, Mulvihill EE, Longuet C, et al.** GLP-1 receptor activation indirectly reduces hepatic lipid accumulation but does not attenuate development of atherosclerosis in diabetic male ApoE$^{-/-}$ mice. *Endocrinology*. 2013;154:127–139.
8. **Körner M, Stöckli M, Waser B, Reubi JC.** GLP-1 receptor expression in human tumors and human normal tissues: potential for in vivo targeting. *J Nucl Med*. 2007;48:736–743.
9. **Madsen LW, Knauf JA, Gotfredsen C, et al.** GLP-1 receptor agonists

and the thyroid: C-cell effects in mice are mediated via the GLP-1 receptor and not associated with RET activation. *Endocrinology*. 2012;153:1538–1547.
10. **Heller RS, Kieffer TJ, Habener JF.** Insulinotropic glucagon-like peptide I receptor expression in glucagon-producing α-cells of the rat endocrine pancreas. *Diabetes*. 1997;46:785–791.
11. **Xu G, Kaneto H, Lopez-Avalos MD, Weir GC, Bonner-Weir S.** GLP-1/exendin-4 facilitates β-cell neogenesis in rat and human pancreatic ducts. *Diabetes Res Clin Pract*. 2006;73:107–110.
12. **Tornehave D, Kristensen P, Rømer J, Knudsen LB, Heller RS.** Expression of the GLP-1 receptor in mouse, rat, and human pancreas. *J Histochem Cytochem*. 2008;56:841–851.
13. **Gier B, Matveyenko AV, Kirakossian D, Dawson D, Dry SM, Butler PC.** Chronic GLP-1 receptor activation by exendin-4 induces expansion of pancreatic duct glands in rats and accelerates formation of dysplastic lesions and chronic pancreatitis in the $Kras^{G12D}$ mouse model. *Diabetes*. 2012;61:1250–1262.
14. **Michel MC, Wieland T, Tsujimoto G.** How reliable are G-protein-coupled receptor antibodies? *Naunyn Schmiedebergs Arch Pharmacol*. 2009;379:385–388.
15. **Pradidarcheep W, Stallen J, Labruyère WT, Dabhoiwala NF, Michel MC, Lamers WH.** Lack of specificity of commercially available antisera against muscarinergic and adrenergic receptors. *Naunyn Schmiedebergs Arch Pharmacol*. 2009;379:397–402.
16. **Pradidarcheep W, Labruyère WT, Dabhoiwala NF, Lamers WH.** Lack of specificity of commercially available antisera: better specifications needed. *J Histochem Cytochem*. 2008;56:1099–1111.
17. **Beermann S, Seifert R, Neumann D.** Commercially available antibodies against human and murine histamine H_4-receptor lack specificity. *Naunyn Schmiedebergs Arch Pharmacol*. 2012;385:125–135.
18. **Pyke C, Knudsen LB.** The glucagon-like peptide-1 receptor—or not? *Endocrinology*. 2013;154:4–8.
19. **Runge S, Schimmer S, Oschmann J, et al.** Differential structural properties of GLP-1 and exendin-4 determine their relative affinity for the GLP-1 receptor N-terminal extracellular domain. *Biochemistry*. 2007;46:5830–5840.
20. **Scrocchi LA, Brown TJ, MaClusky N, et al.** Glucose intolerance but normal satiety in mice with a null mutation in the glucagon-like peptide 1 receptor gene. *Nat Med*. 1996;2:1254–1258.
21. **Bjerre Knudsen L, Madsen LW, Andersen S, et al.** Glucagon-like peptide-1 receptor agonists activate rodent thyroid C-cells causing calcitonin release and C-cell proliferation. *Endocrinology*. 2010;151:1473–1486.
22. **Knudsen LB, Hastrup S, Underwood CR, Wulff BS, Fleckner J.** Functional importance of GLP-1 receptor species and expression levels in cell lines. *Regul Pept*. 2012;175:21–29.
23. **Strobel O, Rosow DE, Rakhlin EY, et al.** Pancreatic duct glands are distinct ductal compartments that react to chronic injury and mediate Shh-induced metaplasia. *Gastroenterology*. 2010;138:1166–1177.
24. **Ruck P, Horny HP, Kaiserling E.** Immunoreactivity of human tissue mast cells: nonspecific binding of primary antibodies against regulatory peptides by ionic linkage. *J Histochem Cytochem*. 1990;38:859–867.
25. **Reubi JC, Perren A, Rehmann R, et al.** Glucagon-like peptide-1 (GLP-1) receptors are not overexpressed in pancreatic islets from patients with severe hyperinsulinaemic hypoglycaemia following gastric bypass. *Diabetologia*. 2010;53:2641–2645.
26. **Gore AC.** Editorial: antibody validation requirements for articles published in endocrinology. *Endocrinology*. 2013;154:579–580.
27. **Drucker DJ.** Incretin action in the pancreas: potential promise, possible perils, and pathological pitfalls. *Diabetes*. 2013;62:3316–3323.
28. **Moreno C, Mistry M, Roman RJ.** Renal effects of glucagon-like peptide in rats. *Eur J Pharmacol*. 2002;434:163–167.
29. **Crajoinas RO, Oricchio FT, Pessoa TD, et al.** Mechanisms mediating the diuretic and natriuretic actions of the incretin hormone glucagon-like peptide-1. *Am J Physiol Renal Physiol*. 2011;301:F355–F363.
30. **Thomson SC, Kashkouli A, Singh P.** Glucagon-like peptide-1 receptor stimulation increases GFR and suppresses proximal reabsorption in the rat. *Am J Physiol Renal Physiol*. 2012;304:F137–F144.
31. **Mundil D, Cameron-Vendrig A, Husain M.** GLP-1 receptor agonists: A clinical perspective on cardiovascular effects. *Diab Vasc Dis Res*. 2012;9:95–108.
32. **Skov J, Dejgaard A, Frøkiaer J, Holst JJ, Jonassen T, Rittig S, Christiansen JS.** Glucagon-like peptide-1 (GLP-1): effect on kidney hemodynamics and renin-angiotensin-aldosterone system in healthy men. *J Clin Endocrinol Metab*. 2013;98:E664–E671.
33. **Kim M, Platt MJ, Shibasaki T, et al.** GLP-1 receptor activation and Epac2 link atrial natriuretic peptide secretion to control of blood pressure. *Nat Med*. 2013;19:567–575.
34. **Tang-Christensen M, Larsen PJ, Göke R, et al.** Central administration of GLP-1-(7–36) amide inhibits food and water intake in rats. *Am J Physiol*. 1996;271:R848–856.
35. **Orskov C, Poulsen SS, Møller M, Holst JJ.** Glucagon-like peptide I receptors in the subfornical organ and the area postrema are accessible to circulating glucagon-like peptide I. *Diabetes*. 1996;45:832–835.
36. **Wettergren A, Schjoldager B, Mortensen PE, Myhre J, Christiansen J, Holst JJ.** Truncated GLP-1 (proglucagon 78–107-amide) inhibits gastric and pancreatic functions in man. *Dig Dis Sci*. 1993;38:665–673.